

Genomic identification and in vitro reconstitution of a complete biosynthetic pathway for the osmolyte di- myo-inositol-phosphate

Dmitry A. Rodionov, Oleg V. Kurnasov, Boguslaw Stec, Yan Wang, Mary F. Roberts, and Andrei L. Osterman

PNAS published online Mar 2, 2007;
doi:10.1073/pnas.0609279104

This information is current as of March 2007.

Supplementary Material

Supplementary material can be found at:
www.pnas.org/cgi/content/full/0609279104/DC1

This article has been cited by other articles:
www.pnas.org/otherarticles

E-mail Alerts

Receive free email alerts when new articles cite this article - sign up in the box at the top right corner of the article or [click here](#).

Rights & Permissions

To reproduce this article in part (figures, tables) or in entirety, see:
www.pnas.org/misc/rightperm.shtml

Reprints

To order reprints, see:
www.pnas.org/misc/reprints.shtml

Notes:

Genomic identification and *in vitro* reconstitution of a complete biosynthetic pathway for the osmolyte di-*myo*-inositol-phosphate

Dmitry A. Rodionov^{*†}, Oleg V. Kurnasov^{*}, Boguslaw Stec^{*}, Yan Wang[‡], Mary F. Roberts[‡], and Andrei L. Osterman^{*§¶}

^{*}Burnham Institute for Medical Research, La Jolla, CA 92037; [‡]Merkert Chemistry Center, Boston College, Chestnut Hill, MA 02467; and [†]Institute for Information Transmission Problems, Russian Academy of Sciences, Moscow 127994, Russia; and [§]Fellowship for Interpretation of Genomes, Burr Ridge, IL 60527

Edited by Emil C. Gotschlich, The Rockefeller University, New York, NY, and approved January 5, 2007 (received for review October 19, 2006)

Di-*myo*-inositol 1,1'-phosphate (DIP) is a major osmoprotecting metabolite in a number of hyperthermophilic species of archaea and bacteria. Although the DIP biosynthesis pathway was previously proposed, genes encoding only two of the four required enzymes, inositol-1-phosphate synthase and inositol monophosphatase, were identified. In this study we used a comparative genomic analysis to predict two additional genes of this pathway (termed *dipA* and *dipB*) that remained missing. In *Thermotoga maritima* both candidate genes (in an originally misannotated locus TM1418) form an operon with the inositol-1-phosphate synthase encoding gene (TM1419). A predicted inositol-monophosphate cytidylyltransferase activity was directly confirmed for the purified product of *T. maritima* gene *dipA* cloned and expressed in *Escherichia coli*. The entire DIP pathway was reconstituted in *E. coli* by cloning of the TM1418–TM1419 operon in pBAD expression vector and confirmed to function in the crude lysate. ³¹P NMR and MS analysis revealed that DIP synthesis proceeds via a phosphorylated DIP intermediate, P-DIP, which is generated by the *dipB*-encoded enzyme, now termed P-DIP synthase. This previously unknown intermediate is apparently converted to the final product, DIP, by an inositol monophosphatase-like phosphatase. These findings allowed us to revise the previously proposed DIP pathway. The genomic survey confirmed its presence in the species known to use DIP for osmoprotection. Among several newly identified species with a postulated DIP pathway, *Aeropyrum pernix* was directly proven to produce this osmolyte.

comparative genomics | di-*myo*-inositol-1,3-phosphate biosynthesis | *Thermotoga maritima*

The most common mechanism of osmoadaptation in microorganisms involves the accumulation of specific organic osmolytes, so-called compatible solutes, amino acids, sugars, and polyols, that can be taken up from the environment or synthesized *de novo* (1–3). In thermophiles and hyperthermophiles, compatible solutes are generally different from those found in mesophiles (4), and many of them additionally contribute to thermoprotection.

Di-*myo*-inositol 1,1'-phosphate (DIP) is one of the major compatible solutes in a number of thermophilic archaea of the genera *Pyrococcus*, *Methanococcus*, *Thermococcus*, and *Archaeoglobus* and bacteria belonging to the genera *Aquifex*, *Rubrobacter*, and *Thermotoga*, including *Thermotoga maritima* and *Thermotoga neapolitana* (4–7). DIP levels are highly increased at supraoptimal growth temperatures in both *Methanococcus igneus* and *Thermotogales*, suggesting that this solute also plays a thermoprotective role (6, 8).

Based on the study in *M. igneus* (9) and the reported stereochemistry of DIP (10), the pathway of DIP biosynthesis was originally proposed to occur in four steps: (i) synthesis of L-*myo*-inositol-1-phosphate (L-I-1-P) from glucose-6-phosphate by NAD⁺-dependent L-I-1-P synthase [inositol-1-phosphate synthase (IPS)]; (ii) hydrolysis of some of the L-I-1-P by inositol monophosphatase (IMP); (iii) coupling of the L-I-1-P with CTP to form CDP-inositol by CTP:inositol monophosphate cytidylyltransferase

(IMPCT); and (iv) generation of DIP by condensation of CDP-inositol with inositol via a DIP synthase (DIPS).

Two of these enzymes, IPS and IMP, are not solely committed to DIP biosynthesis as inositol derivatives play an important role in cell wall biogenesis, signaling, and other pathways in a broad spectrum of species including animals, plants, fungi, and mesophilic bacteria (11–13). Both enzymes are broadly conserved, and examples of each have been well characterized biochemically and structurally, including IMP and IPS from the hyperthermophiles *Methanocaldococcus jannaschii* (14), *Archaeoglobus fulgidus* (15–19), *T. maritima* (20), and *Thermococcus kodakaraensis* (21).

However, two additional enzymes required for DIP biosynthesis have not yet been identified in any organism (3). We used a subsystems-based comparative genomic analysis [as implemented in the SEED platform (22)] to explore the DIP biosynthesis pathway (further termed DIP pathway) in thermophilic species with completely sequenced genomes. Analysis of chromosomal clustering and co-occurrence profiles implicated two previously uncharacterized genes (termed *dipA* and *dipB*; see Fig. 1A) as candidates for the two missing genes of the DIP pathway. Both representative genes from *T. maritima* were cloned and expressed in *Escherichia coli*. The *in vitro* reconstitution of the entire pathway in the crude lysate of *E. coli* and the analysis of the individual enzymatic steps revealed the role of each gene in the DIP pathway. Whereas the *dipA* gene was confirmed to encode a predicted IMPCT enzyme, the product of the *dipB* gene involved in the next step of the pathway appeared to generate a previously unknown phosphorylated DIP intermediate (P-DIP) precursor via the condensation of CDP-inositol with L-I-1-P. The existence of this novel enzymatic activity (termed here PDIPS) instead of the previously postulated DIPS suggested a revision to the previously proposed version of the pathway, where the last step is a dephosphorylation of P-DIP by a phosphatase of the IMP family (Fig. 1B).

The comparative genomic analysis of the entire collection of species with completely sequenced genomes integrated in the SEED database (<http://theseed.uchicago.edu/FIG/index.cgi>) confirmed the presence of the DIP pathway in all archaeal and bacterial species where it was previously detected by biochemical methods

Author contributions: O.V.K., B.S., M.F.R., and A.L.O. designed research; D.A.R., O.V.K., B.S., Y.W., and M.F.R. performed research; D.A.R., M.F.R., and A.L.O. analyzed data; and D.A.R., M.F.R., and A.L.O. wrote the paper.

The authors declare no conflict of interest.

This article is a PNAS direct submission.

Abbreviations: DIP, di-*myo*-inositol 1,1'-phosphate; L-I-1-P, L-*myo*-inositol-1-phosphate; DIPS, DIP synthase; IMP, inositol monophosphatase; IMPCT, CTP:inositol monophosphate cytidylyltransferase; IPS, inositol-1-phosphate synthase; PDIPS, P-DIP synthase.

[¶]To whom correspondence should be addressed at: Burnham Institute for Medical Research, 10901 North Torrey Pines Road, La Jolla, CA 92037. E-mail: osterman@burnham.org.

This article contains supporting information online at www.pnas.org/cgi/content/full/0609279104/DC1.

© 2007 by The National Academy of Sciences of the USA

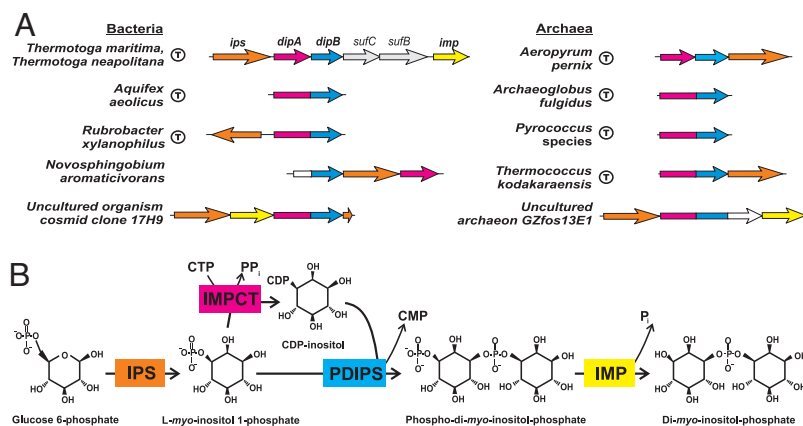


Fig. 1. Reconstruction of the DIP biosynthesis pathway in prokaryotic genomes. (A) Genome context of DIP pathway genes in bacterial and archaeal genomes. (Hyper)thermophilic species are marked by a circle with "T." Orthologs are shown by matching colors of individual genes or respective segments of fused genes. Predicted novel genes (*dipA* and *dipB*) are fused (*dipAB*) or occur in chromosomal clusters with each other and, often, with the two known genes of the DIP pathway (*ips* and *imp*). (B) A diagram of the revised DIP synthesis pathway. IPS, EC 5.5.1.4; IMPCT, 2.7.7.-; PDIPS, 2.7.8.-; IMP, 3.1.3.25.

and allowed us to infer this pathway in several additional microorganisms. Among them, an archaeon *Aeropyrum pernix* was experimentally confirmed to produce this osmolyte.

Results

Prediction of Novel DIP Pathway Genes by Comparative Genomics. Genome context analysis including chromosomal gene clustering, protein fusions, and occurrence profiles were applied to the available genomes of the DIP-producing microorganisms to identify candidate genes for the last two steps of the DIP biosynthesis pathway. The detailed results of this analysis are captured in the SEED subsystem available online (<http://theseed.uchicago.edu/FIG/subsys.cgi>; see "Di-Inositol-Phosphate biosynthesis") and illustrated in Fig. 1 and Table 1.

An observed chromosomal clustering of two previously uncharacterized genes (e.g., *APE1514* and *APE1516* in *A. pernix*) with an *ips* gene (e.g., *APE1517*) in a number of thermophilic archaea and bacteria (Fig. 1A) provided us with the first strong evidence of their possible role in the DIP biosynthesis pathway. In some of these species, the aforementioned genes are colocalized with the *imp* gene, revealing an additional link to this pathway. Moreover, orthologs of these two hypothetical genes (termed here *dipA* and *dipB*) are always either located next to each other on the chromosome or, more often, fused together to form a single gene (*dipAB*), further supporting their strong functional coupling.

An additional scanning of the metagenomic libraries of environ-

mental samples revealed clusters of contiguous *ips*, *imp*, and *dipAB* genes in two uncultured organisms: an archaeon from Eel River sediment from northwestern California and a bacterium from a deep-sea sediment of east Pacific nodule province, China (Fig. 1A).

Additional evidence supporting the possible involvement of these genes in DIP synthesis came from their occurrence only in the genomes containing *ips* and *imp* genes (Table 1). This co-occurrence profile is not in contradiction with the existence of many microbial genomes that contain *ips* and *imp* genes but do not contain *dipA-dipB* genes. For example, in *Mycobacterium tuberculosis* and other actinobacteria IPS plays an essential role in the production of the major inositol-containing thiol and cell wall lipoglycans (23).

Notably, *dipA* and *dipB* genes identified in this study are absent from the current GenBank annotation of the *T. maritima* genome as the respective locus *TM1418* was deemed to contain an authentic frame shift. An alternative interpretation was available in the SEED database (corresponding protein IDs: fig|243274.1.peg.1893 and fig|243274.1.peg.1892 at <http://theseed.uchicago.edu/FIG/index.cgi>) (Fig. 2) suggesting the presence of the two protein-encoding genes (here referred to as *TM1418a* and *TM1418b*) overlapping by 7 bp. Although most species appear to contain a fusion of *dipA* and *dipB* genes within a single reading frame *dipAB*, the existence of two separate genes in *T. maritima* was additionally supported by the presence of single-gene orthologs in *A. pernix* and *Novosphingobium aromaticivorans*.

Table 1. Phylogenetic distribution of the DIP biosynthesis pathway in bacteria and archaea

Organisms	Four-step DIP biosynthesis pathway				DIP production
	IPS	IMPCT	PDIPS	IMP	
<i>T. maritima</i>	TM1419	TM1418a	TM1418b	TM1415	Known
<i>T. neapolitana</i>	020_1986	020_1988	020_1989	020_1993	Known
<i>Aquifex aeolicus</i>	aq.1763	aq.1367 ^N	aq.1367 ^C	aq.1983	Known*
<i>Rubrobacter xylanophilus</i>	Rxyl021258	Rxyl021259 ^N	Rxyl021259 ^C	Rxyl021693	Known
<i>Novosphingobium aromaticivorans</i>	Saro3074	Saro3073	Saro3075	Saro2521	Predicted
Uncultured bacterium 17H9	17H9_20	17H9_22 ^N	17H9_22 ^C	17H9_21	Predicted
<i>A. pernix</i>	APE1517	APE1514	APE1516	APE1798	Confirmed
<i>Ar. fulgidus</i>	AF1794	AF0263 ^N	AF0263 ^C	AF2372	Known
<i>Pyrococcus horikoshii</i>	PH1605	PH1219 ^N	PH1219 ^C	PH1897	Predicted
<i>Pyrococcus abyssi</i>	PAB1989	PAB2433 ^N	PAB2433 ^C	PAB0189	Predicted
<i>Pyrococcus furiosus</i>	PF1616	PF1058 ^N	PF1058 ^C	PF2014	Known
<i>Thermococcus kodakaraensis</i>	TK2278	TK2279 ^N	TK2279 ^C	TK0787	Known*
Uncultured archaeon GZfos13E1	GZ13E1_33	GZ13E1_32 ^N	GZ13E1_32 ^C	GZ13E1_31	Predicted

Genes encoding four enzymes of DIP pathway are shown by standard GenBank identifiers. N and C superscripts denote N-terminal and C-terminal domains in the fusion IMPCT-PDIPS proteins. Organisms experimentally shown to produce DIP are indicated in the last column (4, 7). DIP production in *A. pernix* was predicted and confirmed in this study.

*Cases when DIP production was confirmed in subspecies related to but distinct from those with available genomic sequences.

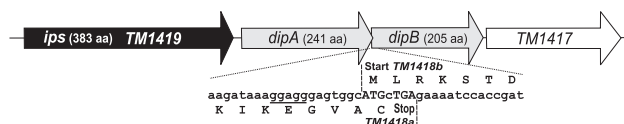


Fig. 2. A reconstructed DIP pathway operon in *T. maritima*. The novel *dipA* and *dipB* genes identified by comparative genomic analysis overlap by 7 bp. Start and stop codons are in capital letters. A possible ribosomal-binding site is underlined.

A long-range homology analysis allowed us to tentatively assign both genes specific functional roles in the DIP synthesis pathway. The *dipA* gene in *T. maritima* encodes a putative 241-aa cytoplasmic protein that belongs to the large family of sugar phosphate nucleotidyltransferases (COG1213). Among characterized members of this protein family are glucose-1-phosphate cytidyltransferase from *Salmonella typhimurium*, 2-C-methyl-D-erythritol 4-phosphate cytidyltransferase from *E. coli*, and mannose-1-phosphate guanylyltransferase from yeast [see supporting information (SI) Fig. 8]. Based on these observations, we tentatively assigned the role of missing IMPCT to the *dipA* gene product.

The *T. maritima dipB* gene encodes a 205-aa protein that belongs to the CDP-alcohol phosphatidyltransferase class-I protein family (COG0558). A BLAST search revealed similarity of DipB to phosphatidylinositol synthases from eukaryotes, phosphatidylglycerophosphate synthases from bacteria, and phosphatidylserine synthases from yeast and bacteria (see SI Fig. 9). This similarity is particularly striking in the region between amino acids 70 and 100, showing a perfect match to the consensus sequence D(X)₂DG(X)₂AR(X)₂N(X)₅G(X)₃D(X)₃D, characteristic of several alcohol phosphatidyltransferases (24). Based on the overall similarity of chemical reactions catalyzed by the previously characterized proteins from the CDP-alcohol phosphatidyltransferase family, we conjectured that DipB is the most likely candidate for the role of the missing DIPS.

Experimental Characterization of Novel DIP Pathway Enzymes from *T. maritima*. To assess the activity of the product of the *T. maritima* gene *dipA* predicted to encode a soluble IMPCT enzyme, this gene was cloned and overexpressed in *E. coli* (see SI Materials and Methods). The recombinant protein with the N-terminal His₆ tag was purified by NiNTA chromatography and enzymatically characterized. Because the product of *T. maritima* gene *dipB* was predicted to be membrane-bound and, hence, insoluble, its activity was tested in a crude lysate of *E. coli* where this gene was expressed as a part of the *T. maritima* operon *ips-dipA-dipB* cloned in the pBAD expression vector. The results of these enzymatic analyses are described in the following subsections. However, so far we failed to express DipB enzyme alone in the active form, which may reflect the importance of an apparent tight association of DipA and DipB proteins (that are more often fused in one polypeptide in other species) for the proper membrane insertion and activity of DipB enzyme.

Enzymatic Characterization of IMPCT. The predicted enzymatic activity of the purified recombinant *T. maritima* IMPCT enzyme was confirmed by the formation of CDP-inositol as characterized by ³¹P NMR spectroscopy and mass spectrometry (MS). The IMPCT reaction converts the CTP and L-I-1-P into CDP-inositol and inorganic pyrophosphate. We used the detection of the latter product for quantitative enzymatic characterization of IMPCT using the coupled colorimetric assay for pyrophosphate. Because of significant substrate inhibition observed at higher concentrations of L-I-1-P (>1 mM), only an estimate of the apparent $K_m \approx 0.2$ mM was obtained for one of its specific substrates, L-I-1-P, at fixed saturating concentration of the second substrate (1.5 mM CTP). With L-I-1-P fixed at 1.0 mM, the V_{max} at 80°C was 160 ± 10 mmol min⁻¹ mg⁻¹, and the apparent K_m for CTP was 0.16 ± 0.04 mM (Fig. 3). The IMPCT appears to be specific for L-inositol-1-phosphate because no CDP-inositol was produced when D-inositol-1-phosphate (Cayman Chemical) was incubated with the recombinant enzyme. This enzyme is also highly selective for CTP because no activity could be detected by the pyrophosphatase coupled assay in the presence of ATP, GTP, or UTP. Moreover, no detectable adduct formation could be detected by ³¹P-NMR spectra even after extensive incubation with any of these alternative NTPs. Deoxy-CTP could serve as a substrate, although the rate was ≈ 20 -fold lower (with 1.5 mM L-I-1-P and 3 mM deoxy-CTP) than with CTP. IMPCT activity was reduced >25-fold in the absence of added MgCl₂, and it was fully suppressed by 5 mM EDTA. These observations confirm the participation of Mg²⁺ in its catalytic mechanism, characteristic of this nucleotidyltransferase family.

Identification of PDIPS Enzyme and Reconstitution of the Entire DIP Pathway. Because the product of the *dipB* gene was expected to be a membrane-protein, its activity was tested in the crude lysate of *E. coli* carrying the operon *ips-dipA-dipB* (TM1419, TM1418a, and TM1418b) from *T. maritima*. This experimental setup allowed us to combine testing of individual enzymatic steps with the pathway reconstitution as none of the respective enzymatic activities or metabolites are present in the *E. coli* host.

The 2,546-bp PCR-amplified segment of *T. maritima* chromosome was cloned into the pBAD-TOPO expression vector and transformed to *E. coli* BL21. The crude cell lysate was obtained after induction with arabinose. Product formation was monitored by ³¹P NMR after incubation with respective substrates at 80°C and compared with available standards and with the samples prepared using the same host strain of *E. coli* carrying the same vector with the β -galactosidase gene as a negative control. The ¹H-coupled ³¹P-NMR analysis of the reaction mixture obtained after incubation of the cell lysate with L-I-1-P and CTP confirmed the formation of CDP-inositol and of a novel phosphodiester compound with a chemical shift similar to that of DIP (Fig. 4). The identity of this compound as P-DIP was later confirmed by MS analysis and by its conversion to DIP upon incubation with an exogenous IMP phosphatase (see below).

The results obtained in this study provided an unambiguous

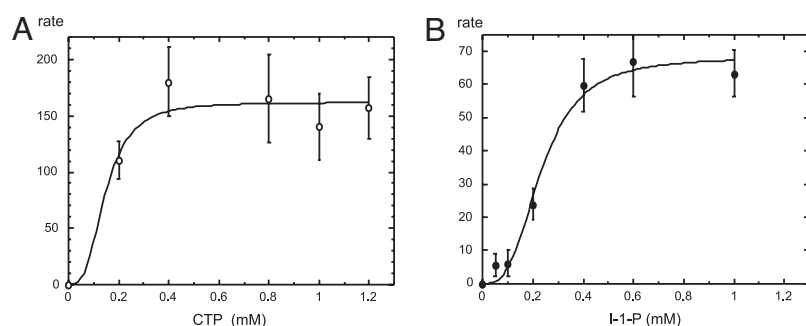
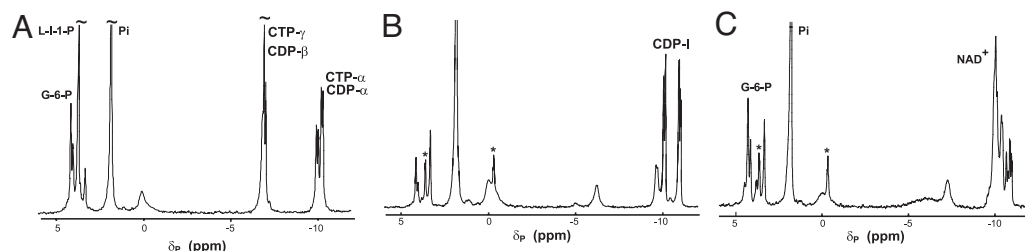


Fig. 3. IMPCT kinetics. (A) Dependence of rate ($\mu\text{mol}\cdot\text{min}^{-1}\cdot\text{mg}^{-1}$) at 80°C for CDP-inositol formation by recombinant IMPCT on CTP concentration with L-I-1-P fixed at 1.0 mM. (B) Dependence of the IMPCT rate on L-I-1-P concentration with the CTP fixed at 1.5 mM. The Mg²⁺ cofactor concentration was 5 mM, and the assay pH was 8.0. Data are shown only up to 1.2 mM substrate because at higher concentrations rates are significantly decreased, suggestive of substrate inhibition. Data were fit with a cooperative model, and $n = 3$ (the average of best fit data for each substrate). The lower specific activities observed for the IMPCT dependence on L-I-1-P is because these rates were acquired with an older preparation of IMPCT.

Fig. 4. ^{31}P NMR (202.2 MHz) ^1H -coupled spectra of soluble fractions from incubations (at 80°C) of *E. coli* BL21-DIP lysed cells with DIP precursors. (A) Control mixture with 3 mM L-I-1-P, 6 mM CTP, 3 mM MgCl_2 , and 6 mM EDTA incubated for 2 h. (B) Lysed cells incubated for 2 h with 3 mM L-I-1-P, 6 mM CTP, and 3 mM MgCl_2 . (C) Lysed cells incubated for 2.5 h with 3 mM glucose-6-phosphate, 1.5 mM NAD^+ , 3 mM CTP, and 3 mM MgCl_2 . After centrifugation of cell debris, EDTA (6 mM) was added to all samples before analysis by ^{31}P NMR spectroscopy. The asterisks indicate the appearance of the DIP-related peaks; the one at -0.2 ppm is the phosphodiester, and the one at ≈ 3 ppm is the phosphomonoester.



assignment of the observed P-DIP synthase (PDIPS) activity to the product of the *dipB* gene as the properties of IPS and IMPCT encoded by the two other genes of the operon were characterized separately (in ref. 17 and in this study, respectively). Addition of the free inositol to the mixture did not lead to any additional formation of DIP, confirming that formation of the P-DIP intermediate via condensation of CDP-inositol with L-I-1-P (and not with free inositol as for a previously postulated DIPS enzyme) is the main and likely the only possible route of DIP synthesis. These findings allowed us to propose a revised version of the DIP pathway shown in Fig. 1B.

Only lysates of cells that contained all three genes of a *T. maritima* DIP operon displayed all of the resonances (including a number of novel peaks) consistent with the proposed pathway and not present in control samples (Fig. 4). Under the conditions used, most of the L-I-1-P was converted to CDP-inositol as monitored by two resonances at -10.2 and -11.0 ppm (each appearing as an AB quartet). Likewise, most of the added CTP was consumed (little intensity for the β -phosphorus remained at -22 ppm, not shown in these graphs). A new triplet resonance appeared at -0.2 ppm, consistent with synthesis of a phosphodiester such as DIP; another new resonance ≈ 4 ppm (a doublet in proton-coupled spectra) consistent with a phosphomonoester had the same integrated intensity as the new phosphodiester peak. The same products in the ^{31}P -NMR spectrum were produced when 3 mM glucose-6-phosphate was incubated with 1.5 mM NAD^+ , 6 mM CTP, and 3 mM MgCl_2 (Fig. 4C), indicating that all three enzymes function under these conditions.

Neither of the two peaks in the ^{31}P -NMR spectra corresponding to CDP-inositol and P-DIP appeared in the absence of Mg^{2+} or in the presence of 6 mM EDTA. In the presence of Mg^{2+} , both of them increased with the time of incubation and exhibited strong temperature dependence. Under our experimental conditions and at the temperatures examined (2 h of incubation at 65, 75, and 85°C), nearly all of the L-I-1-P was converted to CDP-inositol. Activation energy of its conversion to P-DIP is 58 ± 17 kJ/mol, as estimated from the Arrhenius plot (see SI Fig. 10).

Electrospray MS analysis of the reaction mixture revealed two major peaks not present in control samples at 564.2 m/z , consistent with CDP-I, and at 501.2 m/z , consistent with the hypothesized P-DIP (Fig. 5). The peak corresponding to the genuine DIP (421 m/z) appeared only after longer incubation, likely because of the action of endogenous phosphatases. To test the hypothesis that IMP-catalyzed dephosphorylation of the P-DIP precursor may be the last step of the DIP pathway, we first used the exogenous IMP from *M. jannaschii* (25). The samples containing P-DIP were incubated at 85°C with 20 μg of pure recombinant IMP in the presence of an additional 5 mM MgCl_2 (added to offset the EDTA added to obtain ^{31}P spectra that clearly showed P-DIP) for 20 min. The reaction was stopped by cooling and addition of 7 mM EDTA before obtaining a ^{31}P spectrum. This treatment led to the appearance of a new peak 0.2 ppm upfield of the original one (and identical to the resonance of the authentic DIP), accompanied by a dramatic

decrease of the phosphomonoester peak (Fig. 6). Similar results were obtained by using the recombinant IMP-like phosphatase from the *T. maritima* (TM1415) expressed and purified as previously described (20). In this case, all of the P-DIP was converted to DIP under the same incubation conditions.

Interestingly, the formation of both CDP-inositol and P-DIP occurred only when incubation was carried out with an “uncleared” lysate, in suspension containing membrane fragments, consistent with the expectation that PDIPS is an integral membrane protein. The apparent absence of IMPCT activity in the cleared lysate (after removal of cell debris by centrifugation) indicates that this enzyme, perfectly soluble when overexpressed as a single gene, may form a tight complex with membrane-bound PDIPS when expressed as a part of an operon.

Verification of the Predicted DIP Production in *A. pernix*. The comparative genomic analysis allowed us to infer the presence of the DIP pathway in a number of species with completely sequenced genomes where DIP production has not been previously reported (Table 1). To test this conjecture, we checked for DIP production in the hyperthermophilic archaeon *A. pernix*. ^{31}P -NMR spectrum of the ethanol extract of these cells showed one major resonance at -0.3 ppm consistent with DIP, without any indication of P-DIP presence (Fig. 7A). The ^1H NMR spectrum (Fig. 7B) showed resonances consistent with DIP and mannosylglycerate. The identity of the resonances for these two compounds was confirmed by TOCSY and HMQC experiments (6, 26). ^{13}C chemical shifts were obtained from an HMQC experiment and were consistent with published ^{13}C and ^1H shifts for these molecules (27). The MS analysis revealed the presence of 421.2 m/z peak consistent with the DIP anion and the 267.2 m/z peak likely corresponding to mannosylglycerate.

Discussion

Although our current knowledge of major metabolic pathways and respective genes in well studied model bacteria such as *E. coli* is nearly comprehensive, it can be only partially projected on the

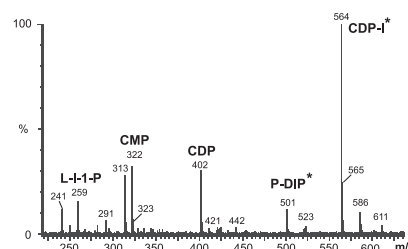


Fig. 5. Mass spectrum of the soluble fraction from incubation (at 80°C) of *E. coli* BL21-DIP lysed cells that had been incubated for 2 h with 3 mM L-I-1-P, 6 mM CTP, and 3 mM MgCl_2 . Identities of the major peaks are indicated. The asterisks highlight ions detected only in spectra from incubations with cell lysates containing the three DIP biosynthetic enzymes IPS, IMPCT, and DIPS.

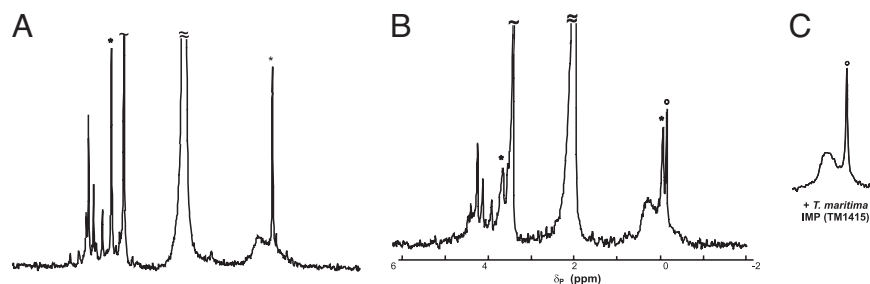


Fig. 6. ^1H -decoupled ^{31}P NMR (202.2 MHz) spectra of the phosphomonoester and phosphodiester region of supernatants from incubation of *E. coli* BL21-DIP lysed cells with L-I-1-P and CTP at 85°C for 2.5 h (A), then treated with *M. jannaschii* IMP (B) or *T. maritima* IMP (C). In A the asterisks mark the new peaks associated with activity of the DIP gene products. Note that IMPase activity reduces the original phosphodiester peak and leads to a new one (marked with \odot) with the same chemical shift as authentic DIP. The DIP-related phosphomonoester peak is also significantly reduced.

rapidly growing number of sequenced genomes of more distant species. Deep-branched bacteria and archaea, including many extremophiles, represent a particular challenge because of a substantial number of unique pathways supporting their divergent lifestyles. In this study we used comparative genomics to address one such challenge and to predict two previously uncharacterized (missing) genes completing the biosynthetic pathway of DIP, a major osmoprotecting metabolite in a number of thermophilic archaea and bacteria (Fig. 1B).

The key evidence implicating two candidate genes termed *dipA* and *dipB* with the DIP pathway was provided by their clustering on the chromosome with the genes encoding IPS and IMP (Fig. 1A), the two previously characterized components of this pathway. Additional support for these conjectures came from the observed co-occurrence profile and a frequent fusion of *dipA* and *dipB* into one contiguous gene *dipAB*. This type of genome context analysis has been successfully applied for identification of missing genes in many metabolic pathways (for review, see ref. 28). General class functions tentatively assigned by homology to the protein products of genes *dipA* (sugar phosphate nucleotidyltransferase, COG1213) and *dipB* (CDP-alcohol phosphatidyltransferase, COG0558) were consistent with their expected functional roles in the DIP pathway.

Enzymatic activities of proteins encoded by the genes *dipA* and *dipB* were experimentally assessed by cloning and expression of the representative genes from *T. maritima*. Remarkably, these missing genes in *T. maritima* were additionally missed at the level of primary gene annotations as the respective chromosomal locus *TM1418* was excluded from the original list of predicted proteins based on the postulated "authentic frame shift." Nevertheless, our results suggest that both protein encoding genes (termed here *TM1418a* and *TM1418b* to preserve the original nomenclature) should be added to the public annotations of the *T. maritima* genome. An overlap of the two adjacent reading frames (Fig. 2) likely reflects a translational coupling often observed for tightly coregulated prokaryotic genes (29).

An enzymatic analysis of the overexpressed and purified product of gene *dipA* (*TM1418a*) confirmed its predicted IMPCT activity, including previously inferred features, such as preference for CTP

over other NTPs and a strict requirement of Mg^{2+} for activity. On the other hand, the analysis of the enzymatic activity of the product of gene *dipB* (*TM1418b*) provided some unexpected results. In keeping with the initial version of the DIP pathway (9), this enzyme was expected to generate DIP by a direct condensation of CDP-inositol (produced from L-I-1-P by IMPCT) with free *myo*-inositol (produced from L-I-1-P by IMP). However, the reconstitution of the pathway in the crude lysate of *E. coli* carrying the entire *ips-dipA-dipB* operon cloned in the expression vector revealed the formation of the previously unknown intermediary metabolite, P-DIP. Therefore, a condensation reaction catalyzed by the product of the *dipB* gene actually involves CDP-inositol and L-I-1-P rather than free inositol. Based on these results, the respective enzyme was termed PDIPS. The last step in the revised version of the DIP pathway is the dephosphorylation of the newly identified intermediate (Fig. 1B). This reaction is likely catalyzed by an IMP-like phosphatase as confirmed by the formation of DIP upon addition of the pure recombinant IMP enzymes from *M. jannaschii* and *T. maritima* to the reaction mixture containing P-DIP.

These findings illustrate a synergy between bioinformatics and experimental aspects of gene discovery. Although the comparative genomics techniques allowed us to accurately predict two novel genes of the DIP pathway, the consequent experimental analysis of the recombinant enzymes was required to confirm one of the inferred activities (IMPCT) and, more importantly, to revise an original prediction of the second activity (PDIPS) and of the entire pathway.

The phylogenetic pattern of occurrence of the DIP pathway genes is in perfect correlation with the previously established distribution of compatible solutes in thermophiles and hyperthermophiles (Table 1). Moreover, projection of the DIP biosynthesis subsystem across the whole collection of integrated complete and almost-complete genomes (http://theseed.uchicago.edu/FIG/subsys.cgi?user=master:&ssa_name=Di-Inositol-Phosphate_biosynthesis&request=show_ssa) allowed us to infer this pathway in seven archaea and six bacteria (including two uncultured species; see Fig. 1A). This inference was further validated in this study by the experimental detection of DIP in the archaeon *A. pernix*. Also in agreement with the available data, DIP pathway signature genes *dipA* and *dipB* are absent from the available genomes of thermophiles where the presence of DIP was not detected in *Thermus thermophilus*, *Pyrobaculum aerophilum*, *Methanopyrus kandleri*, *Sulfolobus solfataricus*, and *Methanobacterium thermoautotrophicum*.

Materials and Methods

Genomes and Bioinformatics Tools. The bulk of comparative genomic analysis, including subsystem encoding and genome context analysis (chromosomal clustering and phylogenetic profiling), was performed by using the SEED genomic database and tools implemented therein (<http://theseed.uchicago.edu/FIG/index.cgi>) (22). Complete and nearly complete genomes of bacteria and archaea were from the GenBank database (www.ncbi.nlm.nih.gov/GenBank). Preliminary genome sequence data for *T. neapolitana* was obtained from The Institute for Genomic Research. We used ClustalX to construct multiple protein alignments (30), Psi-BLAST

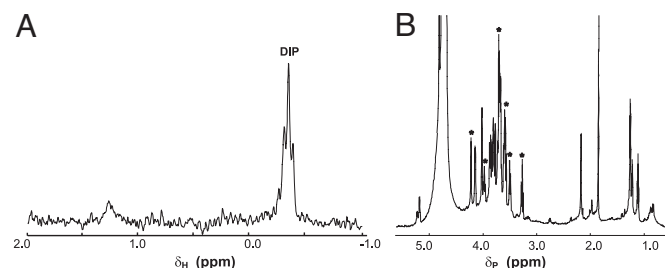


Fig. 7. NMR spectra of *A. pernix* cell extracts. (A) ^{31}P NMR (202.2 MHz) spectrum of an ethanol extract of *A. pernix* JCM 9820. (B) ^1H NMR (202.2 MHz) spectrum of the same extract. ^1H resonances belonging to DIP (determined from a TOCSY spectrum) are indicated by asterisks; other resonances in this extract in the region of DIP belong to mannosylglycerate.

(31) (www.ncbi.nlm.nih.gov/BLAST) to conduct long-range similarity searches, the PFAM (32) (www.sanger.ac.uk/Software/Pfam) and Conserved Domain databases (33) (www.ncbi.nlm.nih.gov/Structure/cdd/cdd.shtml) to identify conserved functional domain, and TMpred (34) (www.ch.embnet.org/software/TMPRED.form.html) to predict the occurrence of transmembrane segments.

Cloning and Expression of *T. maritima* *ips-dipA-dipB* Operon. The 2,546-bp segment containing *ips* and two novel predicted genes, *dipA* and *dipB*, was PCR-amplified by using *T. maritima* MSB8 genomic DNA and oligonucleotide primers ATGgtcaaggtctgctgctcg and TCactgttgtagcaccagaagttc. This fragment was cloned in the pBAD-TOPO expression vector (Invitrogen), and the DNA sequence of the entire fragment was verified. The expression of the operon-encoded genes was performed in *E. coli* strain BL-21 with arabinose induction. Crude cell lysates [0.2 g cells in 1 ml of 50 mM Tris-HCl (pH 7.5)] were heated at 80°C for 5 min to denature most host cell proteins. This suspension was then incubated at 80°C with substrates for DIP synthesis (usually L-I-1-P and CTP but in several instances with glucose-6-phosphate, NAD⁺ as well as CTP) and 3 mM Mg²⁺ for 2–3 h. The sample was cooled to room temperature and centrifuged to remove any cell debris. The supernatant was frozen, lyophilized, and redissolved in D₂O with 6 mM EDTA for NMR studies.

Enzyme Assays. IMPCT activity was assayed by measurement of pyrophosphate production using the EnzChek Pyrophosphate Assay Kit from Invitrogen (35). The recombinant IMPCT (typically 0.5–1.0 mg) was incubated at 80°C with I-1-P (0.2–1.5 mM) and CTP (0.2–1.2 mM) in 100 mM Tris-HCl (pH 8.0) with 5 mM MgCl₂ added, for 0.5, 1, and 2 min. For each time point, the reaction was stopped by placing the sample on ice. The pyrophosphate assay used 50 ml of 20× reaction buffer, 200 ml of 2-amino-6-mercapto-7-methylpurine ribonucleoside as substrate for 10 ml of purine nucleoside phosphorylase, 10 ml of inorganic pyrophosphatase, 530 ml of distilled water, and 200 ml of IMPCT sample. This mixture was incubated at room temperature for 1 h. The absorbance at 360 nm (from the 2-amino-6-mercapto-7-methylpurine) for samples compared with a pyrophosphate standard curve was used to calculate IMPCT-specific activity.

NMR Spectroscopy. Cell extracts were prepared by suspending 0.2 g (wet weight) of cell pellets in 1 ml of 50 mM Tris-HCl (pH 7.5); the suspension was heated to 80°C for 5 min to inactivate most *E. coli* proteins. The suspension was then incubated with 3 mM L-I-1-P that was generated by incubating glucose-6-P in the presence of NAD⁺ (Sigma-Aldrich) and Mg²⁺ with the recombinant IPS from

A. fulgidus at 85°C (15), 6 mM CTP, and 3 mM MgCl₂ at 80°C for 2–2.5 h. The sample was centrifuged at 14,000 rpm for 15 min to pellet all particulate matter. The supernatant was frozen in liquid N₂, lyophilized, and then dissolved in D₂O containing 6 mM EDTA. This soluble extract was examined by ¹H-coupled ³¹P-NMR to assess CDP-inositol and DIP formation (36). All NMR spectra were acquired on a Varian INOVA 500 spectrometer as described previously (9).

Electrospray Mass Spectrometry. Electrospray mass spectrometry of the cell lysates soon after preparation was performed by using negative ion mode in acetonitrile/H₂O, 1:1 with 0.1% ammonia using an LCT Classic spectrometer.

Growing of *A. pernix* for DIP Production. *A. pernix* strain JCM 9820, obtained from the American Type Culture Collection (Manassas, VA), was grown in Difco Marine Broth 2216 to which Na₂S₂O₃·5H₂O (0.1 g per 100 ml of medium) had been added. The medium was inoculated with ice chips of frozen *A. pernix*, and the flasks containing the cells were placed in a shaking water bath at 92°C and 120 rpm (37). After a 30-h lag time, the cells began to grow exponentially (doubling time ≈5–6 h). Cells were harvested after ≈40 h after the lag period when the cells reached OD₆₆₀ ≈0.53; at this point they appeared to be in stationary phase. The cell suspension was centrifuged and the pellet resuspended in 2% NaCl. After centrifugation, the pellet was mixed with 70% ethanol, and the mixture was placed in a bath sonicator for 20 min to ensure lysis of the cells. After centrifugation, the pellet was extracted five times with 70% ethanol and all of the supernatants combined, frozen, and lyophilized. The dried sample was solubilized in D₂O, and both ¹H and ³¹P-NMR spectra were obtained.

Note. When this manuscript was in preparation, Borges *et al.* (38) proposed a similar revision of the DIP pathway based on the detection of the respective enzymatic activities and intermediary metabolites in crude extracts of *A. fulgidus* by NMR. The results of their study are in agreement with the results presented here and confirm that the DIP synthesis occurs via a P-DIP intermediate.

We thank Scott Lesley at the Joint Center for Structural Genomics for providing *T. maritima* chromosomal DNA and Ross Overbeek and the whole team of developers of the SEED genomic platform at the Fellowship for Interpretation of Genomes and Argonne National Laboratory for providing guidance and access to integrated genomes and tools for their comparative analysis. This study was partially supported by the National Institutes of Health Roadmap National Technology Centers on Networks and Pathways Grant 5 U54 RR020843-03, by Department of Energy Biosciences DE-FG02-91ER20025 (to M.F.R.), and by National Institutes of Health Grant 1R01 GM64481 (to B.S.).

- Roberts MF (2004) *Front Biosci* 9:1999–2019.
- Muller V, Spanheimer R, Santos H (2005) *Curr Opin Microbiol* 8:729–736.
- Roberts MF (2005) *Saline Syst* 4:5.
- Santos H, da Costa MS (2001) *Methods Enzymol* 334:302–315.
- Scholz S, Sonnenbichler J, Schafer W, Hensel R (1992) *FEBS Lett* 306:239–242.
- Ciulla RA, Burggraf S, Stettin KO, Roberts MF (1994) *Appl Environ Microbiol* 60:3660–3664.
- Neves C, da Costa MS, Santos H (2005) *Appl Environ Microbiol* 71:8091–8098.
- Martins LO, Carreto LS, Da Costa MS, Santos H (1996) *J Bacteriol* 178:5644–5651.
- Chen L, Spiliotis ET, Roberts MF (1998) *J Bacteriol* 180:3785–3792.
- Van Leeuwen SH, van der Marel GA, Hensel R, van Boom JH (1994) *Recl Trav Chim Pays Bas* 113:335–336.
- Majerus PW (1992) *Annu Rev Biochem* 61:225–250.
- Drobak BK (1992) *Biochem J* 288:697–712.
- Movahedzadeh F, Smith DA, Norman RA, Dinadayala P, Murray-Rust J, Russell DG, Kendall SL, Rison SC, McAlister MS, Bancroft GJ, *et al.* (2004) *Mol Microbiol* 51:1003–1014.
- Stec B, Yang H, Johnson KA, Chen L, Roberts MF (2000) *Nat Struct Biol* 7:1046–1050.
- Chen L, Zhou C, Yang H, Roberts MF (2000) *Biochemistry* 39:12415–12423.
- Stieglitz KA, Johnson KA, Yang H, Roberts MF, Seaton BA, Head JF, Stec B (2002) *J Biol Chem* 277:22863–22874.
- Stieglitz KA, Yang H, Roberts MF, Stec B (2005) *Biochemistry* 44:213–224.
- Neelon K, Wang Y, Stec B, Roberts MF (2005) *J Biol Chem* 280:11475–11482.
- Wang YK, Morgan A, Stieglitz K, Stec B, Thompson B, Miller SJ, Roberts MF (2006) *Biochemistry* 45:3307–3314.
- Chen L, Roberts MF (1999) *Appl Environ Microbiol* 65:4559–4567.
- Sato T, Imanaka H, Rashid N, Fukui T, Atomi H, Imanaka T (2004) *J Bacteriol* 186:5799–5807.
- Overbeek R, Begley T, Butler RM, Choudhuri JV, Chuang HY, Cohoon M, de Crecy-Lagard V, Diaz N, Disz T, Edwards R, *et al.* (2005) *Nucleic Acids Res* 33:5691–5702.
- Jackson M, Crick DC, Brennan PJ (2000) *J Biol Chem* 275:30092–30099.
- Yamashita S, Nikawa J (1997) *Biochim Biophys Acta* 1348:228–235.
- Chen L, Roberts MF (1998) *Appl Environ Microbiol* 64:2609–2615.
- Lamosa P, Martins LO, da Costa MS, Santos H (1998) *Appl Environ Microbiol* 64:3591–3598.
- Silva Z, Borges N, Martins LO, Wait R, da Costa MS, Santos H (1999) *Extremophiles* 3:163–172.
- Osterman A, Overbeek R (2003) *Curr Opin Chem Biol* 7:238–251.
- Eyre-Walker A (1995) *J Bacteriol* 177:5368–5369.
- Thompson JD, Gibson TJ, Plewniak F, Jeanmougin F, Higgins DG (1997) *Nucleic Acids Res* 25:4876–4882.
- Altschul SF, Madden TL, Schaffer AA, Zhang J, Zhang Z, Miller W, Lipman DJ (1997) *Nucleic Acids Res* 25:3389–3402.
- Finn RD, Mistry J, Schuster-Bockler B, Griffiths-Jones S, Hollich V, Lassmann T, Moxon S, Marshall M, Khanna A, Durbin R, *et al.* (2006) *Nucleic Acids Res* 34:D247–D251.
- Marchler-Bauer A, Anderson JB, Cherukuri PF, DeWeese-Scott C, Geer LY, Gwadz M, He S, Hurwitz DI, Jackson JD, Ke Z, *et al.* (2005) *Nucleic Acids Res* 33:D192–D196.
- Hofmann K, Stoffel W (1993) *Biol Chem Hoppe-Seyler* 374:166.
- Upson RH, Haugland RP, Malekzadeh MN, Haugland RP (1996) *Anal Biochem* 243:41–45.
- Roberts MF (2006) *Methods Microbiol* 35:615–647.
- Milek I, Cigic B, Skrt M, Kaletunc G, Ullrich NP (2005) *Can J Microbiol* 51:805–809.
- Borges N, Goncalves LG, Rodrigues MV, Siopa F, Ventura R, Maycock C, Lamosa P, Santos H (2006) *J Bacteriol* 188:8128–8135.